Journal of Medicinal Chemistry

Article

pubs.acs.org/jmc

Development of a Bivalent Dopamine D_2 Receptor Agonist

Julia Kühhorn,[†] Angela Götz,[†] Harald Hübner,[†] Dawn Thompson,[‡] Jennifer Whistler,[‡] and Peter Gmeiner*[,†]

[†]Department of Chemistry and Pharmacy, Emil Fischer Center, Friedrich Alexander University, Schuhstraße 19, D-91052 Erlangen, Germany

[‡]Ernest Gallo Clinic & Research Center and Department of Neurology, University of California, San Francisco, Emeryville, California 94608, United States

Supporting Information

ABSTRACT: Bivalent D_2 agonists may function as useful molecular probes for the discovery of novel neurological therapeutics. On the basis of our recently developed bivalent dopamine D_2 receptor antagonists of type **1**, the bivalent agonist **2** was synthesized when a spacer built from 22 atoms was employed. Compared to the monovalent control compound **6** containing a capped spacer, the bis-aminoindane derivative **2** revealed substantial steepening of the competition curve, indicating a bivalent binding mode. Dimer-specific Hill slopes were not a result of varying functional properties because both the dopaminergic **2** and the monovalent control agent **6** proved to be D_2 agonists substantially inhibiting cAMP accumulation and inducing D_2 receptor internalization. Investigation of the heterobivalent ligands **8** and **9**, containing an agonist and a phenylpiperazine-based antagonist pharmacophore, revealed moderate steepening of the displacement curves and antagonist to very weak partial agonist properties.

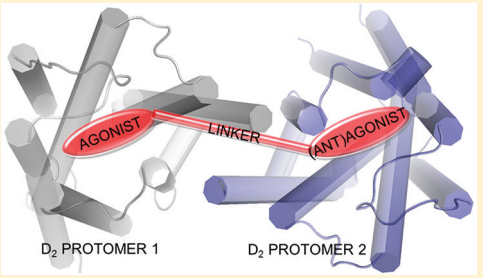

INTRODUCTION

Over the past decade, pharmacological, biochemical, and biophysical evidence has accumulated suggesting that G-protein-coupled receptors (GPCRs) can cross-react to form homo- or heterodimers or higher-order oligomers.[1−3] In some cases, it was shown that dimerization is essential for receptor function and, moreover, can also affect ligand pharmacology, signal transduction, and cellular trafficking.[4,5] Concerning the dopamine D_2 receptor, different studies indicate the existence of homomeric[6−9] and heteromeric complexes.[10,11] According to very recent findings, dopamine D_2 receptor homodimers might be of particular importance in the pathophysiology of schizophrenia.[12] Thus, bivalent antagonists of type **1** can serve as promising pharmacological tools for the discovery of atypical antipsychotics. For the treatment of Parkinsons's disease, dyskinesia, hyperprolactinemia, and restless legs syndrome, D_2-like agonists are needed, suggesting that bivalent agonists may function as useful molecular probes for the development of novel neurological therapeutics.

In a very recent paper, we reported the synthesis and the biological evaluation of type **1** bivalent ligands, incorporating the privileged structure of 1,4-disubstituted aromatic piperidines/piperazines (1,4-DAPs)[13−15] and triazolyl-linked spacer units, differing in length and structure.[16] Radioligand binding assays revealed that the bivalent ligands exhibited a distinct binding profile compared with monovalent control ligands and compounds composed of a pharmacophore with a complete spacer arm and a structurally distorted second pharmacophore. In particular, for the D_2 subtype, some of our bivalent ligands revealed substantial steepening of the competition curve, indicating a bivalent binding mode. This behavior depended on the structure and on the length of the linker arm when the dimeric 1,4-DAP **1** containing a 22-atom spacer gave the steepest curve and a Hill slope of 2.

Taking advantage of these structural insights, we were intrigued by whether bivalent dopamine receptor agonists or partial agonists can be designed in an analogous manner. Competition assays between agonists and radiolabeled antagonists are often characterized by shallow curves with Hill coefficients between 0.5 and 0.7. For the bivalent agonists, a steepening of the competition curves and Hill slopes of at least 1 were expected. The optimized spacer properties and spacer length (22 atoms) should be conserved. However, the pharmacophore should be displaced by structural moieties that were expected to promote agonist properties. *N*-(4-arylcarboxamido)butyl substituted propylaminoindanes are known as strong partial to full D_2 receptor agonists[11,17] and were applied in the present study as agonist pharmacophores of the bivalent ligand **2**. Besides the incorporation of a typical full agonist, we envisioned to investigate bivalent ligands carrying *N*-(4-arylcarboxamido)butyl substituted phenylpiperazines of the class of 1,4-DAPs, which have been described as partial agonists and antagonists.[18−21] In this paper, we describe the synthesis of the homobivalent ligands **2** and **3** and monovalent fragments containing one-half of the linker (Chart 1).

Received: July 25, 2011
Published: October 17, 2011

dx.doi.org/10.1021/jm2009919|*J. Med. Chem.* 2011, 54, 7911−7919

Chart 1. General Approach

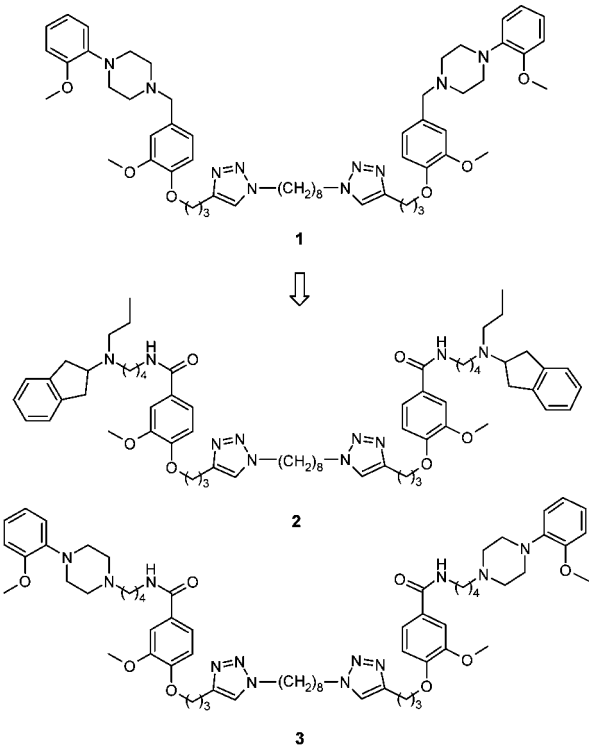

Moreover, heterobivalent ligands, combining agonist and antagonist pharmacophores, are discussed. Diagnostic radioligand binding experiments are also reported revealing Hill slopes that clearly indicated a bivalent binding mode, especially for the bis-aminoindane **2**. Further investigations were directed toward determining dimer specific signaling and internalization properties.

RESULTS AND DISCUSSION

Design. The biological properties of dopaminergic pharmacophores are encoded by an aromatic headgroup, which controls intrinsic activity, and an amine moiety, which is responsible for the formation of a reinforced hydrogen bond to the crucial residue Asp.[3,32] Thus, the *N*-propylaminoindane and the phenylpiperazine scaffolds were chosen to simulate the endogenous biogenic amine.[13] A lipophilic appendage, which is arranged in a defined remote position by a linker unit, was expected to be necessary to enhance ligand affinity. The lipophilic appendage, which is usually represented by a functionalized arene moiety, resides within a hydrophobic microdomain at the extracellular end of TM2, TM3, and TM7 and specifically interacts with residues of the extracellular loop 2 (EL2).[22−24] A formal elongation of the lipophilic moiety is suggested to lead to the "entrance region" of the receptor and from there to the binding pocket of a neighboring protomer. According to our recent findings,[16] the para-position of an aromatic moiety terminating the lipophilic appendage is perfectly applicable as attachment point for a 22-atom spacer.

In various GPCR dimers, interaction interfaces are formed by lipid-exposed surfaces of different TMs, with TM1, TM4, and/or TM5 gaining the most support as dimer interfaces.[25−30] Employing cystein cross-linking experiments, Guo et al.[8,9,31] demonstrated for the dopamine D_2 receptor that TM4/5 forms a symmetrical dimer interface while TM1 and the cytoplasmatic helical domaine H8 are part of a second symmetrical interface. According to the recently established binding mode of the above-described pharmacophores,[20,24] simultaneous interaction of both recognition elements of a bivalent ligand can be accomplished assuming a dopamine D_2 receptor dimer interacting via the TM1/H8 interface. When the human β_2-adrenergic receptor crystal structure[32] was employed as a template, a conceptual dopamine D_2 receptor dimer model was generated with the TM1/H8 interface (Figure 1). Incorporation

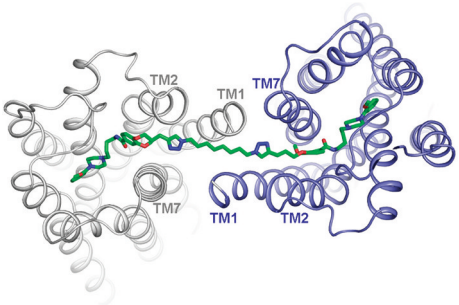

Figure 1. Molecular docking studies demonstrate a potential binding orientation of the bivalent ligand **3** in a D_2 receptor dimer model (top view). A homology model of the human D_{2long} receptor was generated using the human β_2-adrenergic receptor crystal structure as template. The helices TM1 and H8 provide the interface of the D_2 receptor dimer.

of the target compound **3** into the binding pockets of both protomers corroborated our assumption that a bivalent binding mode can be adopted if the 22-atom spacer adopts an extended conformation.

Chemical Synthesis. Homodimeric dopamine receptor ligands with a linker arm built from 22 atoms were synthesized when the spacer length resulted from SAR studies on recently described bivalent GPCR ligands.[33,34] As a dopamine surrogate, we employed *N*-propylaminoindane and *o*-methoxyphenylpiperazine units that were attached via an amidobutyl linker to an arene moiety. For comparative purposes, monovalent fragments containing one-half of the spacer as well as heterobivalent ligands incorporating the *N*-propylaminoindane pharmacophore and a phenylpiperazine-derived pharmacophore of the bivalent ligands **1** and **3** were prepared. To facilitate the introduction of different pharmacophores at the end of a general synthetic route, we intended to proceed via a common intermediate. The synthesis started from methyl vanillate, which was subjected to O-alkylation with 5-chloro-1-pentyne to receive the central building block **4** in 94% yield (Scheme 1). Taking advantage of click chemistry, the preparation of the triazole based precursor of the bivalent target compounds was performed by cooper(I)-catalyzed [3 + 2] azide−alkyne cycloaddition (CuAAC)[35] of 1,8-diazidooctane and the alkyne **4**. Subsequent ester cleavage in the presence of methanolic potassium hydroxide gave access to the carboxylic acid **5**. Finally, HATU-promoted coupling of the molecular scaffold **5** with *N*-propylaminoindanyl or *o*-methoxyphenylpiperazinyl substituted butylamine[17,21] resulted in formation of the bivalent ligands **2** and **3**, respectively, in excellent yields. For the preparation of the monovalent ligands **6** and **7** containing capped spacers, the central building block **4** was reacted with butylazide. Subsequent cleavage of the ester function and amide coupling using TBTU furnished the monovalent products **6** and **7** in 73−83% yield. The synthesis of the heterobivalent probe **8** started again from the alkyne **4**, which was saponified

dx.doi.org/10.1021/jm2009919|*J. Med. Chem.* 2011, 54, 7911−7919

Scheme 1[a]

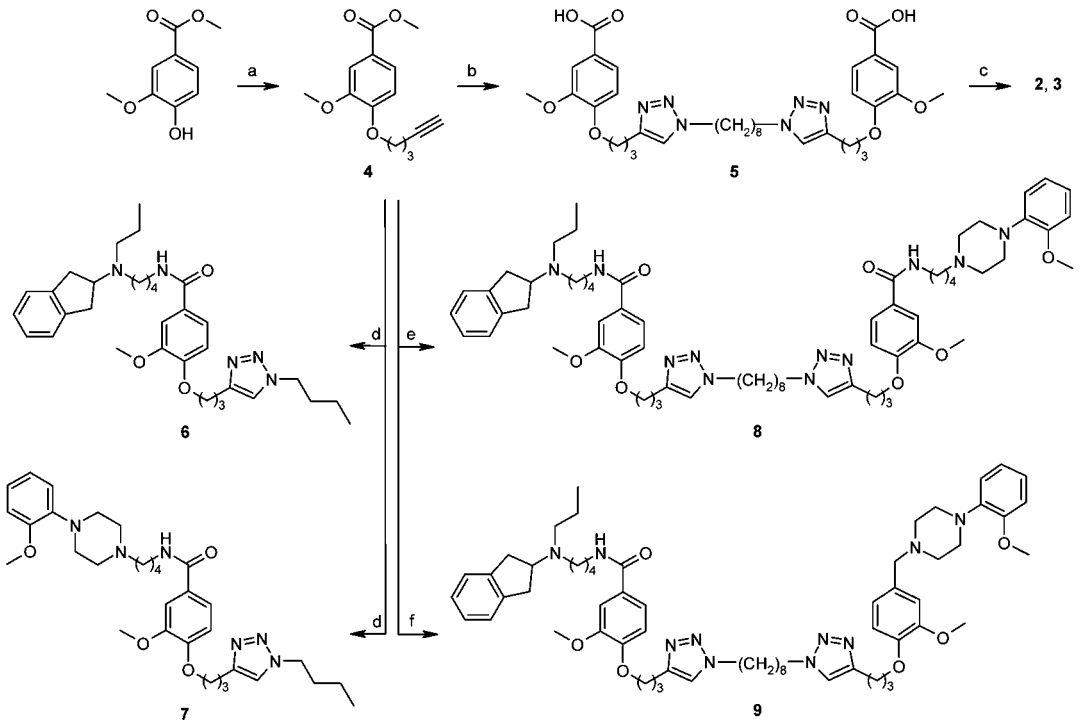

[a]Reagents and conditions: (a) 5-chloro-1-pentyne, K_2CO_3, KI, CH_3CN, reflux, 20 h (94%); (b) (1) 1,8-diazidooctane, sodium ascorbate, $CuSO_4$, 1:4 MeOH/CH_2Cl_2, room temp, 24 h; (2) 2 M KOH, MeOH, 60 °C, 2 h (97%); (c), (*N*-indan-2-yl-*N*-propyl)butan-1,4-diamine or 4-[4-(2-methoxyphenyl)piperazin-1-yl]butan-1-amine, HATU, DIPEA, DMF, 0 °C to room temp, 1−2 h (81−87%); (d) (1) butylazide, sodium ascorbate, $CuSO_4$, 1:2:2 H_2O/^{t}BuOH/CH_2Cl_2, room temp, 16 h (79%); (2) 2 M KOH, MeOH, 60 °C, 2 h (97%); (3) (*N*-indan-2-yl-*N*-propyl)butan-1,4-diamine or 4-[4-(2-methoxyphenyl)piperazin-1-yl]butan-1-amine, TBTU, DIPEA, DMF, CH_2Cl_2, 0 °C to room temp, 20 h (73−83%); (e) (1) 2 M KOH, MeOH, 60 °C, 1.5 h (89%); (2) (*N*-indan-2-yl-*N*-propyl)butan-1,4-diamine or 4-[4-(2-methoxyphenyl)piperazin-1-yl]butan-1-amine, TBTU, DIPEA, DMF, CH_2Cl_2, 0 °C to room temp, 16 h (86−97%); (3) *N*-[4-[indan-2-yl(propyl)amino]butyl]-3-methoxy-4-(pent-4-yn-1-yloxy)benzamide, 1,8-diazidooctane, sodium ascorbate, $CuSO_4$, 1:4 MeOH/CH_2Cl_2, room temp, 2 h (28%); (4) 3-methoxy-*N*-[4-[4-(2-methoxyphenyl)piperazin-1-yl]butyl]-4-(pent-4-yn-1-yloxy)benzamide, sodium ascorbate, $CuSO_4$, 1:4 MeOH/CH_2Cl_2, room temp, 16 h (82%); (f) *N*-[4-[indan-2-yl(propyl)amino]butyl]-3-methoxy-4-(pent-4-yn-1-yloxy)benzamide, 1-[4-[3-[1-(8-azidooctyl)-1*H*-1,2,3-triazole-4-yl]propoxy]-3-methoxyphenyl)methyl]-4-(2-methoxyphenyl)piperazine, sodium ascorbate, $CuSO_4$, 1:4 MeOH/CH_2Cl_2, room temp, 3 h (74%).

and coupled to *N*-propylaminoindanyl substituted butylamine. The resulting intermediate was subjected to CuAAC using a 5-fold excess of 1,8-diazidooctane to afford a triazole derivative incorporating one pharmacophore in 28% yield. Subsequent cycloaddition with the phenylpiperazinylbutyl based pharmacophore equivalent afforded the heterobivalent ligand **8**. Synthesis of the heterobivalent ligand **9** proceeded via an intermediate containing a phenylpiperazinylmethyl-derived pharmacophore[14] when the final triazole formation was performed using an excess of the appropriately functionalized aminoindane pharmacophore.

Receptor Binding. In vitro binding affinity of the homo- and heterobifunctional molecular probes[36−39] along with their monovalent control agents and the reference drug haloperidol was measured by displacement of the radioligand [^{3}H]-spiperone from D_{2long}, D_{2short}, D_3, and $D_{4.4}$ receptors stably expressed in Chinese hamster ovary cells (CHO). D_1 receptor binding affinities were determined utilizing striatal membranes and the D_1 selective radioligand [^{3}H]SCH 23390. The characterization of the test compounds was initiated by carefully comparing the homobivalent ligands **2** and **3** with their monovalent counterparts **6** and **7**. The aminoindane derivatives **2** and **6** gave significant specific binding for D_{2long}, D_{2short}, D_3, and D_4 and clearly reduced D_1 affinity (Table 1). For both variants of the D_2 subtype, K_i values in the double-digit nanomolar range were observed for the bivalent test compound **2** (K_i = 16 nM). K_i values of 1.8 and 0.71 nM for **2** and **6**, respectively, indicated that D_3 binding was high for both the dimeric and the monomeric ligand. The binding pattern observed for the bivalent amidobutylphenylpiperazine **3** displayed 6- to 9-fold lower receptor binding for D_{2long}, D_{2short}, D_3, and D_4 compared to the monovalent analogue **7**.

In the course of our investigations of bivalent GPCR ligands, we also intended to evaluate the pharmacological properties of heterobivalent dopamine receptor ligands, combining an agonist with an antagonist/partial agonist pharmacophore. Thus, dopamine receptor binding studies of the heterobivalent ligands **8** and **9** clearly revealed significant receptor recognition with K_i between 8.8 and 25 nM for the D_2-like subtypes. To gain diagnostic insights into the binding mode of our bivalent test compounds, we analyzed the profiles of the competition curves in detail. Competitive binding curves that follow the law of mass action have a slope of 1. A Hill slope (n_H) less than 1 is considered a reflection of negative cooperativity or the ability of a ligand to bind to G-protein-precoupled receptors with higher affinity than uncoupled receptors. Thus, competition assays between agonists and radiolabeled antagonists are often characterized by shallow curves with Hill coefficients between 0.5 and 0.7. Antagonists tend to have Hill slope values close to 1, since they fail to differentiate between the precoupled and

dx.doi.org/10.1021/jm2009919|*J. Med. Chem.* 2011, 54, 7911−7919

Table 1. Receptor Binding Data for the Bivalent Compounds 1−3, 8, 9 and the Monomeric Controls 6, 7, 10 in Comparison to the Reference Haloperidol Employing Porcine Dopamine D_1 Receptor and the Human Subtypes D_{2long}, D_{2short}, D_3, and $D_{4.4}$

		K_i [a] ± SEM (nM) and Hill slope [b] (absolute value of n_H ± SEM)					
		[^{3}H]SCH 23390	[^{3}H]spiperone				
compd	composition	pD_1	hD_{2long}	hD_{2short}	hD_3	$hD_{4.4}$
2	homobi "6 + 6"	510 ± 67	16 ± 1.1 [1.3 ± 0.06]	16 ± 2.5 [1.3 ± 0.2]	1.8 ± 0.43 [1.5 ± 0.1]	34 ± 3.2 [1.4 ± 0.1]
3	homobi "7 + 7"	2800 ± 550	110 ± 21 [1.2 ± 0.1]	110 ± 19 [1.1 ± 0.06]	12 ± 5.4 [1.3 ± 0.2]	660 ± 140 [1.0 ± 0.08]
1	homobi "10 + 10"	220 ± 61	22 ± 2.4 [2.0 ± 0.1]	41 ± 8.2 [2.0 ± 0.1]	84 ± 11 [1.6 ± 0.1]	15 ± 1.3 [1.6 ± 0.1]
6	mono	6000 ± 550	12 ± 1.9 [0.5 ± 0.02]	4.1 ± 0.62 [0.6 ± 0.02]	0.71 ± 0.083 [0.9 ± 0.04]	42 ± 3.6 [0.8 ± 0.04]
7	mono	1200 ± 100	17 ± 3.2 [0.8 ± 0.05]	12 ± 2.5 [0.8 ± 0.06]	2.0 ± 0.34 [0.9 ± 0.05]	84 ± 12 [0.9 ± 0.03]
10 [c]	mono	1500 ± 140	67 ± 12 [1.1 ± 0.0]	53 ± 11 [1.0 ± 0.1]	610 ± 190 [1.2 ± 0.2]	7.2 ± 1.3 [1.0 ± 0.1]
8	heterobi "6 + 7"	200 ± 19	25 ± 7.1 [1.5 ± 0.06]	17 ± 3.4 [1.5 ± 0.1]	2.0 ± 0.20 [1.4 ± 0.09]	40 ± 2.9 [1.3 ± 0.10]
9	heterobi "6 + 10"	330 ± 25	14 ± 2.4 [1.2 ± 0.07]	8.8 ± 1.1 [1.0 ± 0.07]	1.2 ± 0.25 [1.6 ± 0.2]	22 ± 5.3 [1.2 ± 0.05]
haloperidol		93 ± 11	1.5 ± 0.44 [1.0 ± 0.1]	1.1 ± 0.16 [1.1 ± 0.1]	6.3 ± 1.6 [1.1 ± 0.1]	6.3 ± 1.3 [1.2 ± 0.1]

[a] K_i ± SEM derived from 4 to 19 experiments each done in triplicate. [b] Hill slopes ± SEM are derived from the same binding curves recorded for the determination of K_i values; the original n_H was negative but is displayed as absolute value. [c] **10**: 1-[[4-[3-(1-butyl-1*H*-1,2,3-triazol-4-yl)propoxy]-3-methoxyphenyl]methyl]-4-(2-methoxyphenyl)piperazine.

the uncoupled receptor population, thereby following the general law of mass action for single site competition.[40] For the bivalent ligand **1**, a steepening of the competition curves was observed, compared to the respective monomer, leading to a Hill slope of 2.0 for the interactions with D_{2long} and D_{2short}. This is indicative of a positive cooperative binding, which is usually observed as an allosteric effect inducing a conformational crosstalk within one receptor protomer or modulation of the interaction between two protomers of a receptor dimer.[41,42] Bivalent ligands addressing two adjacent binding sites of receptor dimers will also induce such cooperativity because bivalent binding of the second pharmacophore is significantly accelerated because of the vicinity of ligand and the thus facilitated enrichment of local concentration. Thus, bivalent binding leads to the liberation of 2 equiv of radioligand and a substantial steepening of the competition curve. Examination of the binding curves of the monomeric ligand **6** at D_{2long} and D_{2short} revealed shallow Hill slopes between 0.5 and 0.6, indicating agonistic properties. Interestingly, careful analysis of the competition experiments that we conducted with the dimeric analogue **2** revealed steepening of the competition curves. Hill slopes of 1.3 were calculated for the interaction of D_{2long} and D_{2short} with the bivalent ligand **2** (Figure 2).

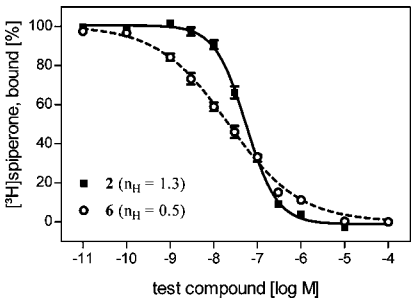

Figure 2. Representative binding curves of the homobivalent ligand **2** and its monovalent control agent **6** at the human D_{2long} receptor displaying different curve shapes resulting in Hill slopes (absolute value of n_H) of 1.3 (for **2**) and 0.5 (for **6**) indicating a bivalent and a monovalent binding mode, respectively.

Two different hypotheses can be formulated to explain the steepening of the competition curve: (1) a claim that the bis-aminoindane **2** exhibits a bivalent binding mode, leading to the liberation of 2 equiv of radioligand, or (2) a change of functional activity from the monovalent ligand **6** to the bivalent ligand **2** from agonist to antagonist properties. To gain further insights, functional experiments determining the activation profiles of **6** and **2** were envisioned.

In contrast to the results obtained for the aminoindane derivatives, the Hill slope of the bivalent phenylpiperazine **3** (n_H = 1.0−1.3) differs only slightly from the value for the monovalent control ligand **7** (n_H = 0.8−0.9), which may be a result of a coexistence of binding modes displacing 1 equiv of [^{3}H]spiperone and those liberating 2 equiv of radioligand. Analyses of the heterobivalent ligand **8** revealed a steepening of the competition curves (n_H = 1.5 at D_{2long} and D_{2short}) compared to their monovalent building blocks **6** and **7** (n_H = 0.5−0.8), while the heterobivalent ligand **9** gave Hill slopes close to 1 for the interaction with D_{2long} and D_{2short}. Interestingly, a strongly increased Hill coefficient of 1.6 was calculated for the interaction of **9** with D_3 when compared to

Table 2. Intrinsic Activity of the Bivalent Compounds 1−3, 8, 9 and the Monomeric Controls 6, 7, 10 Determined at the D_{2long} Receptor by Measuring the Inhibition of cAMP Accumulation and the Propensity To Induce Internalization in Comparison with the Reference Compound Quinpirole

	compd								
	2	**3**	**1**	**6**	**7**	**10**[g]	**8**	**9**	quinpirole
cAMP[a]									
Eff[b]	84 ± 8.3	<3[d]	<3[d]	88 ± 4.2	<3[d]	<3[d]	<3[d]	13 ± 5.6	101 ± 0.87
EC_{50}[c]	440 ± 64			13 ± 6.3				380 ± 120	140 ± 45
internalization[e]	+	−	−	+	−	−	−	−	+
Hill slope (n_H)[f]	1.3 ± 0.06	1.2 ± 0.1	2.0 ± 0.1	0.5 ± 0.02	0.8 ± 0.05	1.1 ± 0.0	1.5 ± 0.06	1.2 ± 0.07	

[a]Bioluminescence based cAMP-Glo assay using a D_{2long} expressing CHO cell line. [b]Ligand efficacy ± SEM in % compared to the full agonist quinpirole. [c]EC_{50} ± SEM in nM derived from the mean curves of three to nine experiments each done in triplicate. [d]Data from two independent experiments done in triplicate. [e]Ligand effects on D_{2long} receptor internalization: + = ligand stimulates receptor internalization; − = no ligand mediated receptor internalization. [f]Hill slopes ± SEM are derived from binding curves recorded for the determination of K_i values (Table 1); the original n_H was negative but is displayed as absolute value. [g]**10**: 1-[[4-[3-(1-butyl-1*H*-1,2,3-triazol-4-yl)propoxy]-3-methoxyphenyl]methyl]-4-(2-methoxyphenyl)piperazine.

the values of the monovalent fragment **6** (n_H = 0.9) and the respective monovalent ligand of **1** (1-[[4-[3-(1-butyl-1*H*-1,2,3-triazol-4-yl)propoxy]-3-methoxyphenyl]methyl]-4-(2-methoxyphenyl)piperazine, **10**), which contains one-half of the linker (n_H = 1.2).

Functional Experiments. To better understand the biological properties of our bivalent dopaminergics, intrinsic activities of the ligands were determined by measuring the ability of the test compounds to modulate D_{2long} receptor mediated inhibition of cAMP accumulation and to induce internalization of FLAG-tagged D_{2long} receptors.[43]

When a bioluminescence based cAMP assay was employed, substantial D_2 agonist activity was observed for the bivalent ligand **2** and its monovalent control agent **6** with 84% and 88% ligand efficacy, respectively (Table 2). A significantly higher EC_{50} value was calculated for **2** compared to **6**, indicating that the bivalent binding requires a higher receptor occupation to exert signaling. On the other hand, the phenylpiperazinylmethyl substituted ligands **1** and **10**, incorporating an antagonist pharmacophore, as well as the phenylpiperazinylbutyl derivatives **3** and **7** were not able to inhibit cAMP accumulation.

The test compounds were evaluated for their propensity to induce internalization of the FLAG-tagged D_{2long} receptor. In agreement with the outcome of the cAMP accumulation assay, the homobivalent ligands **1** and **3** as well as the corresponding monomers **10** and **7** were not able to induce D_2 internalization, whereas the aminoindane derivatives **2** and **6** potently induced translocation of the receptor from the plasma membrane to the cytosol, indicating receptor internalization (Figure 3). The heterobivalent ligands **8** and **9** linking an agonist with an antagonist pharmacophore were also investigated for their ability to induce activation and internalization. Measuring the inhibition of cAMP accumulation revealed D_2 antagonist behavior for **8** and low partial agonist properties for **9** (eff = 13%). Both heterobivalent test compounds did not induce D_2 receptor internalization. Obviously, recognition of the phenylpiperazine derived antagonist moieties of the heterobivalent ligands leads to an inhibition of D_2 internalization and ligand efficacy of the aminoindane pharmacophore. Thus, for this series, there did not appear to be a functional dissociation or "ligand bias" for cAMP accumulation versus receptor internalization at saturating ligand concentration. However, while both dimers **2** and **9** had similar potencies for cAMP accumulation, the heterodimer **9** was not able to induce receptor internalization, suggesting that at physiological doses within a native system with lower D_2 expression levels, the heterodimer **9** might be less likely to cause down-regulation of the D_2 receptor via internalization,[43] which has been shown to be important for regulating the balance of D_1 and D_2 receptor signaling in vivo.[44]

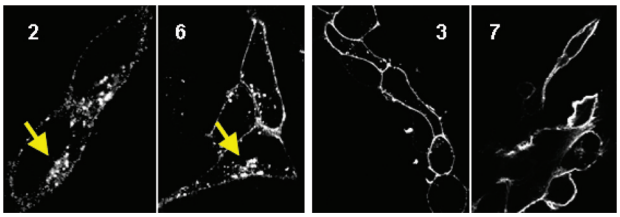

Figure 3. Ligand induced D_{2long} receptor internalization. FLAG-tagged D_{2long} receptors stably expressed in HEK293 cells were incubated with M1 antibody followed by treatment for 30 min with **2**, **3**, **6**, and **7** each at 10 μM. Treatment with **2** and **6** potently induced D_{2long} receptor internalization (indicated with yellow arrow). No internalization was observed after incubation with **3** and **7**. Representative pictures of each condition are shown (n = 3).

CONCLUSION

On the basis of our recently developed bivalent dopamine D_2 receptor antagonists of type **1**, the bivalent agonist **2** was developed. Compared with monovalent control compounds containing capped spacers, both ligands revealed substantial steepening of the competition curve, indicating a bivalent binding mode. Dimer-specific Hill slopes were not a result of varying functional properties because both the dopaminergic **2** and the monovalent control agent **6** were able to substantially inhibit cAMP accumulation and to induce D_2 receptor internalization. Investigation of the heterobivalent ligands **8** and **9**, containing an agonist and a phenylpiperazine-based antagonist pharmacophore, revealed moderate steepening of the displacement curves and antagonist to very weak partial agonist properties in both functional assays. Thus, recognition of the phenylpiperazine derived antagonist moieties of the heterobivalent ligands leads to an inhibition of D_2 internalization and ligand efficacy of the aminoindane pharmacophore indicating functional crosstalk between two physically interacting D_2 protomers.

dx.doi.org/10.1021/jm2009919|*J. Med. Chem.* 2011, 54, 7911–7919

EXPERIMENTAL SECTION

Chemistry. Dry solvents and reagents were of commercial quality and were used as purchased. MS were run on a JEOL JMS-GC Mate II spectrometer by EI (70 eV) with solid inlet or a Bruker Esquire 2000 by APC or ionization. HR-EIMS experiments were run on a JEOL JMS-GC Mate II using Peak-Matching ($M/\Delta M > 5000$). NMR spectra were obtained on a Bruker Avance 360 or a Bruker Avance 600 spectrometer relative to TMS in the solvents indicated (J in Hz). Melting points were determined with a MEL-TEMP II melting point apparatus (Laboratory Devices, U.S.) in open capillaries and given uncorrected. IR spectra were performed on a Jasco FT/IR 410 spectrometer. Purification by flash chromatography was performed using silica gel 60; TLC analyses were performed using Merck 60 F254 aluminum sheets and analyzed by UV light (254 nm). Analytical HPLC was performed on Agilent 1100 HPLC systems employing a VWL detector. As column, a ZORBAX ECLIPSE XDB-C18 (4.6 mm × 150 mm, 5 μm) was used. HPLC purity was measured using following binary solvent systems: system A, eluent, CH_3OH in 0.1% aqueous trifluoroacetic acid, 10−100% CH_3OH in 15 min, 100% for 3 min, flow rate of 1.0 mL/min, λ = 254 nm; system B, eluent, CH_3CN in 0.1% aqueous trifluoroacetic acid, 10% CH_3CN for 2 min to 95% CH_3CN in 18 min, 95% for 1 min, flow rate of 1.0 mL/min, λ = 254 nm. The purity of all test compounds and key intermediates was determined to be >95%.

Methyl 3-Methoxy-4-(pent-4-yn-1-yloxy)benzoate (4). A suspension of methyl 4-hydroxy-3-methoxybenzoate (4.0 g, 22.0 mmol), 5-chloropent-1-yne (5.86 mL, 54.9 mmol), K_2CO_3 (9.1 g, 65.9 mmol), and KI (3.6 g, 22.0 mmol) in anhydrous CH_3CN (60 mL) was stirred at reflux temperature for 20 h. Then the reaction mixture was allowed to cool to room temperature, and the solvent was evaporated. The residue was dissolved in H_2O and extracted with CH_2Cl_2. The combined organic layers were dried ($MgSO_4$) and evaporated. The residue was purified by flash chromatography (hexane/EtOAc, 4:1 to 2:1) to give **4** as a white solid (5.13 g, 94% yield), mp 67 °C. IR 3277, 2951, 1714, 1601, 1515, 1435, 1295, 1272, 1222, 1134, 1033, 762 cm^{-1}. ^1H NMR (360 MHz, $CDCl_3$) δ 1.98 (t, J = 2.7 Hz, 1H), 2.08 (m, 2H), 2.43 (dt, J = 6.9, 2.7 Hz, 2H), 3.89 (s, 3H), 3.91 (s, 3H), 4.18 (t, J = 6.4 Hz, 2H), 6.91 (d, J = 8.4 Hz, 1H), 7.55 (d, J = 2.0 Hz, 1H), 7.65 (dd, J = 8.4, 2.0 Hz, 1H). ^{13}C NMR (150 MHz, $CDCl_3$) δ 15.1, 27.9, 51.9, 56.0, 67.2, 69.0, 83.2, 111.7, 112.4, 122.7, 123.5, 148.9, 152.4, 166.9. HPLC system A (254 nm) purity 97% (t_R = 13.6 min); system B (254 nm) purity 98% (t_R = 15.2 min). HR-EIMS calcd m/z for $C_{14}H_{16}O_4$, 248.1049; found 248.1049.

4,4′-[Octane-1,8-diylbis(1*H*-1,2,3-triazol-1,4-diylpropan-3,1-diyloxy)]bis(3-methoxybenzoic acid) (5). A suspension of **4** (500 mg, 2.0 mmol), 1,8-diazidooctane[45] (200 mg, 1.0 mmol), sodium ascorbate (60 mg, 0.3 mmol), and copper sulfate pentahydrate (25 mg, 0.1 mmol) in MeOH (3 mL) and CH_2Cl_2 (12 mL) was stirred at room temperature overnight. The reaction was quenched with saturated aqueous $NaHCO_3$ and 0.1 M EDTA, extracted with CH_2Cl_2, dried (Na_2SO_4), and evaporated. The residue was dissolved in a methanolic solution of KOH (10 mL, 2M). The resulting solution was stirred at 60 °C for 2 h. Then MeOH was evaporated. The residue was adjusted to pH 1 with 2 M HCl and extracted with a mixture of CH_2Cl_2 and MeOH (3:1). The organic layer was dried (Na_2SO_4) and evaporated. The residue was purified by flash chromatography (CH_2Cl_2/MeOH, 95:5 to 92:8 + 0.5% TFA) to give **5** as a white solid (652.4 mg, 97% yield), mp 187 °C. IR 2929, 1670, 1581, 1516, 1467, 1423, 1271, 1226, 1028, 766 cm^{-1}. ^1H NMR (360 MHz, DMSO-d_6) δ 1.13−1.25 (m, 8H), 1.75 (m, 4H), 2.06 (m, 4H), 2.77 (t, J = 7.6 Hz, 4H), 3.81 (s, 6H), 4.07 (t, J = 6.4 Hz, 4H), 4.27 (t, J = 7.2 Hz, 4H), 7.01 (d, J = 8.3 Hz, 2H), 7.45 (d, J = 1.9 Hz, 2H), 7.53 (dd, J = 8.3, 1.9 Hz, 2H), 7.88 (s, 2H). ^{13}C NMR (150 MHz, DMSO-d_6) δ 21.6, 25.7, 28.2, 28.4, 29.6, 49.1, 55.5, 67.5, 111.9, 112.2, 121.8, 123.06, 123.14, 146.0, 148.4, 151.9, 167.1. APCI-MS calcd m/z for $C_{34}H_{44}N_6O_8$, 664.7; found 665 $(M + H)^+$.

4,4′-[Octane-1,8-diylbis(1*H*-1,2,3-triazol-1,4-diylpropan-3,1-diyloxy)]bis[*N*-[4-[indan-2-yl(propyl)amino]butyl]-3-methoxybenzamide] (2). A solution of **5** (30 mg, 45 μmol) in anhydrous DMF (2 mL) was cooled to 0 °C before a solution of HATU (69 mg, 181 μmol) in anhydrous DMF (1 mL) was added. The reaction mixture was stirred for 10 min. Then DIPEA (22 μL, 135 μmol) was added very slowly, and after that a solution of (*N*-indan-2-yl-*N*-propyl)butane-1,4-diamine[17] (28 mg, 113 μmol) in anhydrous DMF (2 mL) was added dropwise. The mixture was stirred for 1 h at room temperature before aqueous $NaHCO_3$ was added. The aqueous layer was extracted with CH_2Cl_2. Then the combined organic layers were washed three times with brine, dried (Na_2SO_4), and evaporated. The residue was purified by flash chromatography (CH_2Cl_2/MeOH, 98:2 to 96:4 + 0.5% TEA) to give **2** as a colorless oil (44.1 mg, 87% yield). IR 2933, 1637, 1547, 1506, 1462, 1269, 1225, 1128, 1030, 744 cm^{-1}. ^1H NMR (600 MHz, $CDCl_3$) δ 0.87 (t, J = 7.4 Hz, 6H), 1.22−1.32 (m, 8H), 1.49 (m, 4H), 1.55−1.68 (m, 8H), 1.76−1.90 (m, 4H), 2.23 (m, 4H), 2.50 (m, 4H), 2.57 (t, J = 7.2 Hz, 4H), 2.87 (dd, J = 15.1, 8.7 Hz, 4H), 2.92 (t, J = 7.4 Hz, 4H), 3.00 (dd, J = 15.5, 7.9 Hz, 4H), 3.45 (m, 4H), 3.65 (m, 2H), 3.89 (s, 6H), 4.06 (t, J = 6.4 Hz, 4H), 4.28 (t, J = 7.0 Hz, 4H), 6.57 (m, 2H), 6.77 (d, J = 8.3 Hz, 2H), 7.09−7.17 (m, 8H), 7.21 (dd, J = 8.3, 1.9 Hz, 2H), 7.30 (s, 2H), 7.42 (d, J = 1.9 Hz, 2H). ^{13}C NMR (150 MHz, $CDCl_3$) δ 12.0, 19.8, 22.1, 25.0, 26.2, 27.8, 28.7, 30.2, 40.1, 50.1, 51.0, 53.3, 56.1, 63.0, 67.9, 111.1, 111.7, 119.2, 120.9, 124.4, 126.3, 127.6, 141.7, 147.0, 149.3, 151.0, 167.2. HPLC system A (254 nm) purity >99% (t_R = 12.1 min); system B (254 nm) purity 98% (t_R = 12.7 min). APCI-MS calcd m/z for $C_{66}H_{92}N_{10}O_6$, 1121.5; found 1122 $(M + H)^+$.

Radioligand Binding Studies. Receptor binding studies were carried out as described previously.[46] In brief, competition binding experiments with the human D_{2long}, D_{2short}, D_3, and $D_{4.4}$ receptors were run on membrane preparations from CHO cells stably expressing the corresponding receptor. Assays were run with membranes at protein concentrations per well of 1−10 μg/mL and [^{3}H]spiperone (specific activity of 84 Ci/mmol, PerkinElmer, Rodgau, Germany) at final concentrations of 0.1−0.4 nM according to the individual K_D values in binding buffer (50 mM Tris, 1.0 mM EDTA, 5.0 mM $MgCl_2$, 100 μg/mL bacitracin, and 5 μg/mL soybean trypsin inhibitor at pH 7.4). The K_D values were 0.040−0.18, 0.090−0.24, 0.10−0.36, and 0.15−0.30 nM for the D_{2long}, D_{2short}, D_3, and D_4 receptor, respectively. The corresponding B_{max} values were in the range of 450−1270 fmol/mg for D_{2long}, 675−2595 fmol/mg for D_{2short}, 1450−11080 fmol/mg for D_3, and 565−1810 fmol/mg for D_4 receptor. Nonspecific binding was determined in the presence of 10 μM haloperidol. Specific binding represented about 85% of the total binding. The D_1 receptor binding experiments were performed with homogenates prepared from porcine striatum as described.[46] Assays were run with membranes at protein concentrations per well of 20−40 μg/mL and radioligand concentrations of 0.3−0.5 nM [^{3}H]SCH 23390 (specific activity of 60 Ci/mmol, Biotrend, Köln, Germany) with K_D values of 0.51−0.67 nM. Protein concentration was established by the method of Lowry using bovine serum albumin as a standard.[47]

Adenylyl Cyclase Inhibition Assay. Bioluminescence based cAMP-Glo assay (Promega, Mannheim, Germany) was performed according to the manufacturer's instructions. Briefly, CHO cells expressing D_{2long} receptor were seeded into a white half-area 96-well plate (5000 cells/well) 24 h prior to the assay. On the days of the assays, cells were washed with phosphate buffered saline (PBS, pH 7.4) to remove traces of serum and incubated with various concentrations of compounds in the presence of 20 μM forskolin in serum-free medium that contained 500 μM IBMX and 100 μM Ro 20-1724, pH 7.4. After 15 min of incubation at 25 °C, cells were lysed with cAMP-Glo lysis buffer, kinase reaction was performed with a reaction buffer containing PKA, and finally an equal volume of Kinase-Glo reagent was added. Bioluminescence was read on a microplate reader Victor^{3}V (Perkin-Elmer, Rodgau, Germany). The experiments were performed two to nine times per compound with each concentration in triplicate.

Data Analysis. The resulting competition curves of the receptor binding experiments and activity assay were analyzed by nonlinear regression using the algorithms in PRISM 5.0 (GraphPad Software, San Diego, CA). Competition curves were fitted to a sigmoid curve by nonlinear regression analysis in which the log EC_{50} and the Hill

coefficient were free parameters. EC_{50} values were transformed to K_i values according to the equation of Cheng and Prusoff.[48]

Immunocytochemistry. The antibody-feeding immunocytochemistry experiments were performed as described.[49] Briefly, cells stably expressing FLAG-tagged D_{2long} receptor were grown on coverslips pretreated with gelatin to ~50% confluency. Live cells were fed M1 antibody (Sigma) directed against the FLAG epitope (1:1000, 30 min) and then incubated with ligands (10 μM, 30 min) or left untreated. Cells were then fixed with 4% formaldehyde in PBS, pH 7.4. After fixation, cells were permeabilized in Blotto (3% milk, 0.1% Triton X, 1 mM $CaCl_2$, 50mM Tris·HCl, pH 7.5) and stained with Alexa Fluor 594 or Alexa Fluor 488 goat anti-mouse IgG2b antibody (Invitrogen, 1:500, 45 min). The coverslips were mounted using mounting medium from Vectashield. Images were acquired at 63× with a LSM 510 laser confocal microscope (Zeiss) or a TCS SP5 confocal microscope (Leica Microsystems). Confocal images were exported as TIFF files and processed using GIMP 2.6.

Construction of the Dopamine D_2 Receptor Dimer. The previously published homology model of the dopamine D_2 receptor[24] was used to construct a dopamine D_2 dimer. The model was built using the crystal structure of the β_2-adrenergic receptor[32] as a template. The dimeric arrangement of two monomers was accomplished according to Guo et al.[9] The dimer was constructed by means of VMD[50] and afterward submitted to energy minimization in order to avoid repulsive interactions between proximate amino acid side chains. Therefore, the SANDER classic module of AMBER 10[51] was used by applying 500 cycles of steepest descent minimization, followed by 4500 cycles of conjugate gradient minimization. The calculation was carried out in a water box with periodic boundary conditions and a nonbonded cutoff of 8.0 Å. The all atom force field ff99SB was applied.[52] The minimized receptor dimer was used for the insertion of a bivalent ligand.

Insertion of a Bivalent Ligand into the Dopamine D_2 Receptor Dimer. The *N*-(4-phenylcarboxamido)butyl substituted phenylpiperazine moieties of the bivalent ligand **3** were inserted into both receptor monomers based on the recently published receptor–ligand complexes[20,24] and connected via a triazole linker. The linker was built using Sybyl 6.9[53] and following energy minimized by means of the Tripos force field[54] and Gasteiger–Hückel charges,[55,56] which are implemented in Sybyl 6.9. The linker is positioned between TM2 and TM7 in both monomers, which enables the simultaneous interaction of the bivalent ligand with both monomers.

■ ASSOCIATED CONTENT

Ⓢ Supporting Information

Detailed reaction scheme for the synthesis of the mono- and heterobivalent target compounds (**6**–**9**), experimental and spectroscopic data of the nonkey target compounds **3** and **6**–**9** and the respective precursors thereof, receptor binding data employing porcine 5-HT_1, 5-HT_2, and α_1 receptors, confocal images of the antibody-feeding immunocytochemistry experiments after stimulation with quinpirole, with the compounds **1** and **8**–**10**, or with no ligand added. This material is available free of charge via the Internet at http://pubs.acs.org.

■ AUTHOR INFORMATION

Corresponding Author

*Phone: +49 9131 85-29383. Fax: +49 9131 85-22585. E-mail: peter.gmeiner@medchem.uni-erlangen.de.

■ ACKNOWLEDGMENTS

We thank Prof. Thomas Stamminger (Institute for Clinical and Molecular Virology, University of Erlangen-Nuremberg, Germany) for providing the confocal microscope and Dr. Nuska Tschammer for conducting microscopy experiments. This research was funded by a grant of the Deutsche Forschungsgemeinschaft (DFG: Gm 13/8).

■ ABBREVIATIONS USED

GPCR, G-protein-coupled receptor; 1,4-DAP, 1,4-disubstituted aromatic piperidine/piperazine; TM, transmembrane domain; EL, extracellular loop; CuAAC, copper(I)-catalyzed azide–alkyne cycloaddition; TBTU, 2-(1*H*-benzotriazole-1-yl)-1,1,3,3-tetramethyluronium tetrafluoroborate; HATU, 2-(7-aza-1*H*-benzotriazole-1-yl)-1,1,3,3-tetramethyluronium hexafluorophosphate; CHO, Chinese hamster ovary; HEK, human embryonic kidney; K_i, inhibition constant; SEM, standard error of the mean; n_H, Hill slope; HR-EIMS, high resolution electron ionization mass spectrometry; APCI-MS, atmospheric pressure chemical ionization mass spectrometry

■ REFERENCES

(1) George, S. R.; O'Dowd, B. F.; Lee, S. P. G-protein-coupled receptor oligomerization and its potential for drug discovery. *Nat. Rev. Drug Discovery* **2002**, *1*, 808–820.

(2) Milligan, G. G protein-coupled receptor dimerization: function and ligand pharmacology. *Mol. Pharmacol.* **2004**, *66*, 1–7.

(3) Smith, N. J.; Milligan, G. Allostery at G protein-coupled receptor homo- and heteromers: uncharted pharmacological landscapes. *Pharmacol. Rev.* **2010**, *62*, 701–725.

(4) Milligan, G. G protein-coupled receptor dimerisation: molecular basis and relevance to function. *Biochem. Biophys. Acta* **2007**, *1768*, 825–835.

(5) Milligan, G. A day in the life of G protein-coupled receptor: the contribution to function of G protein-coupled receptor dimerization. *Br. J. Pharmacol.* **2008**, *153*, 216–229.

(6) Vivo, M.; Lin, H.; Strange, P. G. Investigation of cooperativity in the binding of ligands to the dopamine D_2 receptor. *Mol. Pharmacol.* **2006**, *69*, 226–235.

(7) Ng, G. Y. N.; O'Dowd, B.; Lee, S. P.; Chung, H. T.; Brann, M. R.; Seeman, P.; George, S. R. Dopamine D2 receptor dimers and receptor-blocking peptides. *Biochem. Biophys. Res. Commun.* **1996**, *227*, 200–204.

(8) Guo, W.; Shi, L.; Filizola, M.; Weinstein, H.; Javitch, J. A. Crosstalk in G protein-coupled receptors: changes at the transmembrane homodimer interface determine activation. *Proc. Natl. Acad. Sci. U.S.A.* **2005**, *102*, 17495–17500.

(9) Guo, W.; Urizar, E.; Kralikova, M.; Mobarec, J. C.; Shi, L.; Filizola, M.; Javitch, J. A. Dopamine D2 receptors form higher order oligomers at physiological expression levels. *EMBO J.* **2008**, *27*, 2293–2304.

(10) Rocheville, M.; Lange, D. C.; Kumar, U.; Patel, S. C.; Patel, R. C.; Patel, Y. C. Receptors for dopamine and somatostatin: formation of hetero-oligomers with enhanced functional activity. *Science* **2000**, *288*, 154–157.

(11) Koschatzky, S.; Tschammer, N.; Gmeiner, P. Cross-receptor interactions between dopamine D2L and neurotensin NTS1 receptors modulate binding affinities of dopaminergics. *ACS Chem. Neurosci.* **2011**, *2*, 308–316.

(12) Wang, M.; Pei, L.; Fletcher, P. J.; Kapur, S.; Seeman, P.; Liu, F. Schizophrenia, amphetamine-induced sensitized state and acute amphetamine exposure all show a common alteration: increased dopamine D2 receptor dimerization. *Mol. Brain* **2010**, *3*, 25.

(13) Löber, S.; Hübner, H.; Tschammer, N.; Gmeiner, P. Recent advances in the search for D3- and D4-selective drugs: probes, models and candidates. *Trends Pharmacol. Sci.* **2011**, *32*, 148–157.

(14) Kulagowski, J. J.; Broughton, H. B.; Curtis, N. R.; Mawer, I. M.; Ridgill, M. P.; Baker, R.; Emms, F.; Freedman, S. B.; Marwood, R.; Patel, S.; Patel, S.; Ragan, C. I.; Leeson, P. D. 3-[[4-(4-Chlorophenyl)-piperazin-1-yl]-methyl]-1*H*-pyrrolo[2,3-b]pyridine: an antagonist with high affinity and selectivity for the human dopamine D4 receptor. *J. Med. Chem.* **1996**, *39*, 1941–1942.

(15) Haubmann, C.; Hübner, H.; Gmeiner, P. 2,2-Dicyanovinyl as a nonaromatic aryl bioisostere: synthesis, binding experiments and SAR

studies of highly selective dopamine D4 receptor ligands. *Bioorg. Med. Chem. Lett.* **1999**, *9*, 1969−1972.
(16) Kühhorn, J.; Hübner, H.; Gmeiner, P. Bivalent dopamine D2 receptor ligands: synthesis and binding properties. *J. Med. Chem.* **2011**, *54*, 4896−4903.
(17) Tschammer, N.; Dörfler, M.; Hübner, H.; Gmeiner, P. Engineering a GPCR−ligand pair that simulates the activation of D2L by dopamine. *ACS Chem. Neurosci.* **2010**, *1*, 25−35.
(18) Huber, D.; Hübner, H.; Gmeiner, P. 1,1′-Disubstituted ferrocenes as molecular hinges in mono- and bivalent dopamine receptor ligands. *J. Med. Chem.* **2009**, *52*, 6860−6870.
(19) Tschammer, N.; Bollinger, S.; Kenakin, T.; Gmeiner, P. Histidine 6.55 is a major determinant of ligand-based signaling in dopamine D2L receptor. *Mol. Pharmacol.* **2011**, *79*, 575−585.
(20) Tschammer, N.; Elsner, J.; Goetz, A.; Ehrlich, K.; Schuster, S.; Ruberg, M.; Kühhorn, J.; Thompson, D.; Whistler, J.; Hübner, H.; Gmeiner, P Highly potent 5-aminotetrahydropyrazolopyridines: enantioselective dopamine D3 receptor binding, functional selectivity, and analysis of receptor−ligand interactions. *J. Med. Chem.* **2011**, *54*, 2477−2491.
(21) Hackling, A.; Robin Ghosh, R.; Perachon, S.; Mann, A.; Höltje, H.-D.; Wermuth, C. G.; Schwartz, J.-C.; Sippl, W.; Sokoloff, P.; Stark, H. *N*-(ω-(4-(2-Methoxyphenyl)piperazin-1-yl)alkyl)carboxamides as dopamine D_2 and D_3 receptor ligands. *J. Med. Chem.* **2003**, *46*, 3883−3899.
(22) Kortagere, S.; Gmeiner, P.; Weinstein, H.; Schetz, J. A. Certain 1,4-disubstituted aromatic piperidines and piperazines with extreme selectivity for the dopamine D4 receptor interact with a common receptor microdomain. *Mol. Pharmacol.* **2004**, *66*, 1491−1499.
(23) Simpson, M. M.; Ballesteros, J. A.; Chiappa, V.; Chen, J.; Suehiro, M.; Hartman, D. S.; Godel, T.; Snyder, L. A.; Sakmar, T. P.; Javitch, J. A. Dopamine D4/D2 receptor selectivity is determined by a divergent aromatic microdomain contained within the second, third, and seventh membrane-spanning segments. *Mol. Pharmacol.* **1999**, *56*, 1116−1126.
(24) Ehrlich, K.; Götz, A.; Bollinger, S.; Tschammer, N.; Bettinetti, L.; Härterich, S.; Hübner, H.; Lanig, H.; Gmeiner, P. Dopamine D2, D3, and D4 selective phenylpiperazines as molecular probes to explore the origins of subtype specific receptor binding. *J. Med. Chem.* **2009**, *52*, 4923−4935.
(25) Lee, S. P.; O'Dowd, B. F.; Rajaram, R. D.; Nguyen, T.; George, S. R. D2 dopamine receptor homodimerization is mediated by multiple sites of interaction, including an intermolecular interaction involving transmembrane domain 4. *Biochemistry* **2003**, *42*, 11023−11031.
(26) Carrillo, J. J.; Lopez-Gimenez, J. F.; Milligan, G. Multiple interactions between transmembrane helices generate the oligomeric alpha1b-adrenoceptor. *Mol. Pharmacol.* **2004**, *66*, 1123−1137.
(27) Lopez-Gimenez, J. F.; Canals, M.; Pediani, J. D.; Milligan, G. The alpha1b-adrenoceptor exists as a higher-order oligomer: effective oligomerization is required for receptor maturation, surface delivery, and function. *Mol. Pharmacol.* **2007**, *71*, 1015−1029.
(28) Fung, J. J.; Deupi, X.; Pardo, L.; Yao, X. J.; Velez-Ruiz, G. A.; DeVree, B. T.; Sunahara, R. K.; Kobilka, B. K. Ligand-regulated oligomerization of β_2-adrenoceptors in a model lipid bilayer. *EMBO J.* **2009**, *28*, 3315−3328.
(29) Mancia, F.; Assur, Z.; Herman, A. G.; Siegel, R.; Hendrickson, W. A. Ligand sensitivity in dimeric associations of the serotonin 5HT2c receptor. *EMBO Rep.* **2008**, *9*, 363−369.
(30) Overton, M. C.; Chinault, S. L.; Blumer, K. J. Oligomerization, biogenesis, and signaling is promoted by a glycophorin A-like dimerization motif in transmembrane domain 1 of a yeast G protein-coupled receptor. *J. Biol. Chem.* **2003**, *278*, 369−377.
(31) Guo, W.; Shi, L.; Javitch, J. A. The fourth transmembrane segment forms the interface of the dopamine D2 recptor homodimer. *J. Biol. Chem.* **2003**, *278*, 4385−4388.
(32) Cherezov, V.; Rosenbaum, D. M.; Hanson, M. A.; Rasmussen, S. G. F.; Thian, F. S.; Kobilka, T. S.; Choi, H.-J.; Kuhn, P.; Weis, W. I.; Kobilka, B. K.; Stevens, R. C. High-resolution crystal structure of an engineered human β_2-adrenergic G protein-coupled receptor. *Science* **2007**, *318*, 1258−1265.
(33) Bhushan, R. G.; Sharma, S. K.; Xie, Z.; Daniels, D. J.; Portoghese, P. S. A bivalent ligand (KDN-21) reveals spinal delta and kappa opioid receptors are organized as heterodimers that give rise to delta(1) and kappa(2) phenotypes. Selective targeting of delta−kappa heterodimers. *J. Med. Chem.* **2004**, *47*, 2969−2972.
(34) Portoghese, P. S.; Larson, D. L.; Sayre, L. M.; Yim, C. B.; Ronsisvalle, G.; Tam, S. W.; Takemori, A. E. Opioid agonist and antagonist bivalent ligands. The relationship between spacer length and selectivity at multiple opioid receptors. *J. Med. Chem.* **1986**, *29*, 1855−1861.
(35) Rostovtsev, V. V.; Green, L. G.; Fokin, V. V.; Sharpless, K. B. A stepwise Huisgen cycloaddition process: copper(I)-catalyzed regioselective "ligation" of azides and terminal alkynes. *Angew. Chem., Int. Ed.* **2002**, *41*, 2596−2599.
(36) Neumeyer, J. L.; Zhang, A.; Xiong, W.; Gu, X. H.; Hilbert, J. E.; Knapp, B. I.; Negus, S. S.; Mello, N. K.; Bidlack, J. M. Design and synthesis of novel dimeric morphinan ligands for κ and μ opioid receptors. *J. Med. Chem.* **2003**, *46*, 5162−5170.
(37) Zhang, Y.; Gilliam, A.; Maitra, R.; Damaj, M. I.; Tajuba, J. M.; Seltzman, H. H.; Thomas, B. F. Synthesis and biological evaluation of bivalent ligands for the cannabinoid 1 receptor. *J. Med. Chem.* **2010**, *53*, 7048−7060.
(38) Russo, O.; Berthouze, M.; Giner, M.; Soulier, J. L.; Rivail, L.; Sicsic, S.; Lezoualc'h, F.; Jockers, R.; Berque-Bestel, I. Synthesis of specific bivalent probes that functionally interact with 5-HT(4) receptor dimers. *J. Med. Chem.* **2007**, *50*, 4482−4492.
(39) Berque-Bestel, I.; Lezoualc'h, F.; Jockers, R. Bivalent ligands as specific pharmacological tools for G protein-coupled receptor dimers. *Curr. Drug Discovery Technol.* **2008**, *5*, 312−318.
(40) Urban, J. D.; Clarke, W. P.; von Zastrow, M.; Nichols, D. E.; Kobilka, B.; Weinstein, H.; Javitch, J. A.; Roth, B. L.; Christopoulos, A.; Sexton, P. M.; Miller, K. J.; Spedding, M.; Mailman, R. B. Aripiprazole has functionally selective actions at dopamine D2 receptor-mediated signaling pathways. *J. Pharmacol. Exp. Ther.* **2007**, *320*, 1−13.
(41) Smith, N. J.; Milligan, G. Allostery at G-protein-coupled receptor homo- and heteromers: uncharted pharmacological landscapes. *Pharmacol. Rev.* **2010**, *62*, 701−725.
(42) Albizu, L.; Balestre, M. N.; Breton, C.; Pin, J. P.; Manning, M.; Mouillac, B.; Barberis, C.; Durroux, T. Probing the existence of G protein-coupled receptor dimers by positive and negative ligand-dependent cooperative binding. *Mol. Pharmacol.* **2006**, *70*, 1783−1791.
(43) Bartlett, S. E.; Enquist, J.; Hopf, F. W.; Lee, J. H.; Gladher, F.; Kharazia, V.; Waldhoer, M.; Mailliard, W. S.; Armstrong, R.; Bonci, A.; Whistler, J. L. Dopamine responsiveness is regulated by targeted sorting of D2 receptors. *Proc. Natl. Acad. Sci. U.S.A.* **2005**, *102*, 11521−11526.
(44) Thompson, D.; Martini, L.; Whistler, J. L. Altered ratio of D1 and D2 dopamine receptors in mouse striatum is associated with behavioral sensitization to cocaine. *PLoS One* **2010**, *5*, No. e11038.
(45) Thomas, J. R.; Liu, X.; Hergenrother, P. J. Size-specific ligands for RNA hairpin loops. *J. Am. Chem. Soc.* **2005**, *127*, 12434−12435.
(46) Hübner, H.; Haubmann, C.; Utz, W.; Gmeiner, P. Conjugated enynes as nonaromatic catechol bioisosteres: synthesis, binding experiments, and computational studies of novel dopamine receptor agonists recognizing preferentially the D(3) subtype. *J. Med. Chem.* **2000**, *43*, 756−762.
(47) Lowry, O. H.; Rosebrough, N. J.; Farr, A. L.; Randall, R. J. Protein measurement with the folin phenol reagent. *J. Biol. Chem.* **1951**, *193*, 265−275.
(48) Cheng, Y.; Prusoff, W. H. Relationship between the inhibition constant (K_i) and the concentration of inhibitor which causes 50 per cent inhibition (IC_{50}) of an enzymatic reaction. *Biochem. Pharmacol.* **1973**, *22*, 3099−3108.
(49) Finn, A. K.; Whistler, J. L. Endocytosis of the mu opioid receptor reduces tolerance and a cellular hallmark of opiate withdrawal. *Neuron* **2001**, *32*, 829−839.

(50) Humphrey, W.; Dalke, A.; Schulten, K. VMD: Visual Molecular Dynamics. *J Mol. Graphics* **1996**, *14*, 33−38.
(51) Case, D. A.; Darden, T. A.; Cheatham, T. E., III; Simmerling, C. L.; Wang, J.; Duke, R. E.; Luo, R.; Crowley, M.; Walker, R. C.; Zhang, W.; Merz, K. M.; Wang, B.; Hayik, S.; Roitberg, A.; Seabra, G.; Kolossváry, I.; Wong, K. F.; Paesani, F.; Vanicek, J.; Wu, X.; Brozell, S. R.; Steinbrecher, T.; Gohlke, H.; Yang, L.; Tan, C.; Mongan, J.; Hornak, V.; Cui, G.; Mathews, D. H.; Seetin, M. G.; Sagui, C.; Babin, V.; Kollman, P. A. *AMBER 10*; University of California: San Francisco, CA, 2008.
(52) Hornak, V.; Abel, R.; Okur, A.; Strockbine, B.; Roitberg, A.; Simmerling, C. Comparison of multiple amber force fields and development of improved protein backbone parameters. *Proteins: Struct., Funct., Bioinf.* **2006**, *65*, 712−725.
(53) *Sybyl 6.9*; Tripos Inc. (1699 South Hanley Road, St. Louis, Missoury, 63144).
(54) Clark, M.; Cramer, R. D. III; Van Opdenbosch, N. Validation of the general purpose Tripos 5.2 force field. *J. Comput. Chem.* **1989**, *10*, 982−1012.
(55) Gasteiger, J.; Marsili, M. Iterative partial equalization of orbital electronegativity: a rapid access to atomic charges. *Tetrahedron* **1980**, *36*, 3219−3228.
(56) Gasteiger, J.; Marsili, M. A new model for calculating atomic charges in molecules. *Tetrahedron Lett.* **1978**, *19*, 3181−3184.